

2022-7

## Modelling spherical aberration detection in an analog holographic wavefront sensor

Emma Branigan

*Technological University Dublin, emma.branigan@tudublin.ie*

Suzanne Martin

*Technological University Dublin, suzanne.martin@tudublin.ie*

Matthew Sheehan

*Technological University Dublin, matthew.sheehan@tudublin.ie*

*See next page for additional authors*

Follow this and additional works at: <https://arrow.tudublin.ie/cieocon2>



Part of the [Numerical Analysis and Computation Commons](#), and the [Optics Commons](#)

---

### Recommended Citation

E. Branigan, S. Martin, M. Sheehan, and K. Murphy, "Modelling spherical aberration detection in an analog holographic wavefront sensor," in *Imaging and Applied Optics Congress 2022 (3D, AOA, COSI, ISA, pcAOP)*, Technical Digest Series (Optica Publishing Group, 2022), paper OF2B.4. DOI: 10.1364/AOA.2022.OF2B.4

This Conference Paper is brought to you for free and open access by the Centre for Industrial and Engineering Optics at ARROW@TU Dublin. It has been accepted for inclusion in Conference Papers by an authorized administrator of ARROW@TU Dublin. For more information, please contact [arrow.admin@tudublin.ie](mailto:arrow.admin@tudublin.ie), [aisling.coyne@tudublin.ie](mailto:aisling.coyne@tudublin.ie), [gerard.connolly@tudublin.ie](mailto:gerard.connolly@tudublin.ie).



This work is licensed under a [Creative Commons Attribution-NonCommercial-Share Alike 4.0 License](#)  
Funder: Science Foundation Ireland

---

**Authors**

Emma Branigan, Suzanne Martin, Matthew Sheehan, and Kevin Murphy

# Modelling spherical aberration detection in an analog holographic wavefront sensor

Emma Branigan<sup>1</sup>, Suzanne Martin<sup>1</sup>, Matthew Sheehan<sup>2</sup>, Kevin Murphy<sup>1,\*</sup>

1. Centre for Industrial and Engineering Optics, School of Physics & Clinical & Optometric Sciences, TU Dublin

2. School of Physics & Clinical & Optometric Sciences, TU Dublin

\*kevin.p.murphy@tudublin.ie

**Abstract:** The analog holographic wavefront sensor (AHWFS) is a simple and robust solution to wavefront sensing in turbulent environments. Here, the ability of a photopolymer-based AHWFS to detect refractively generated spherical aberration is modelled and verified. © 2022 The Author(s)

## 1. Introduction

### 1.1. Wavefront sensing

Real-time compensation for both low and high order aberrations (e.g. defocus and spherical aberration) can be applied through adaptive optics systems, typically comprised of corrective optics and a wavefront sensor (WFS). The role of the WFS is to detect the magnitude and type of the aberrations present in an incident wavefront and, for many years, has been used as an assistive technology for corrective procedures such as laser refractive surgery [1] and high-resolution imaging in astronomy [2].

When a wavefront containing arbitrary aberration modes is incident on the AHWFS it is optically decomposed into a set of paired diffracted beams [3–5] associated with each mode and are detected by a photodiode array. A simple ratio of intensities, given by Eq. 1 [6], determines the type and magnitude of the aberration. This elegant algorithm for wavefront fitting offers a significant reduction in computational overhead compared to other WFS and its speed is limited only by the chosen photodiode. It also ensures insensitivity to scintillation and obscuration.

$$W_B = \frac{g_-(a) - g_+(a)}{g_-(a) + g_+(a)} \quad (1)$$

### 1.2. A third-order approximation of spherical aberration

Wavefront aberrations can be considered in terms of geometrical ray intercept errors at the image plane [7], or as optical path length differences. Here, we employ the former technique in order to quantify the magnitude of spherical aberration introduced by a series of refractive elements. This treatment of the geometrical aberrations was first published by Ludwig von Seidel and includes all of the third order terms in a centered system of spherical surfaces [8]. Longitudinal spherical aberration (LSA) can be defined as the difference between the paraxial and the marginal foci. LSA can be related to the Seidel aberration coefficient by Eq. 2, where A is the Seidel aberration coefficient,  $\Delta z$  is the magnitude of LSA, R is the reference sphere radius and y is the ray height.

$$A = \frac{\Delta z}{3R^2y^2} \quad (2)$$

## 2. Materials and methods

The reproducibility and chemical post-processing and developing of materials such as silver halide and DCG are some of the major material challenges that can be avoided through recording multiplexed holographic optical elements (HOE) in photopolymers. Here we use a self-developing acrylamide-based photopolymer which is mass producible [9, 10] and has good reproducibility, from one volume hologram to the next, without post-processing.

We have previously shown that various powers of the defocus aberration, within a range of +/-15.0D, can be detected by a photopolymer-based AHWFS [11]. A biconvex refractive lens was recorded holographically to produce two extremes of a sensing range. The result was the separate recording of a holographic converging lens and a holographic diverging lens. Here, in addition to improved results for defocus detection, we seek to extend the sensing capability of the AHWFS to include spherical aberration. First a theoretical model was developed to

investigate the angular selectivity of the recording medium at various layer thicknesses to establish the capability of the device. By changing both the thickness and the central recording spatial frequency, it was possible to tune the sensitivity of the device. A Zemax model of the optical system gave a magnitude of the Seidel aberration coefficient for spherical aberration, from which the LSA was calculated by Eq. 2. Trigonometry was then used to predict the angular shift of the fringes inside the recording medium.

### 3. Results

Two biconvex lenses arranged in a 4f imaging system, with focal lengths of 50mm and 35mm respectively, were modelled with Zemax optical design software at  $\lambda = 532\text{nm}$ . The magnitude of spherical aberration generated by the lens combination was  $0.67\lambda$  or  $2.85\mu\text{m}$ , given in Seidel aberration coefficients (Fig. 1). The LSA was modelled across an entrance beam of 5.7mm in diameter. At the marginal rays,  $\pm 2.85\text{mm}$  in height, the magnitude of  $\Delta z$  was greatest and caused a  $1.69^\circ$  shift off the Bragg reconstruction angle. However, as  $\Delta z \propto y^2$  this shift is notably smaller with a reduction in ray height.

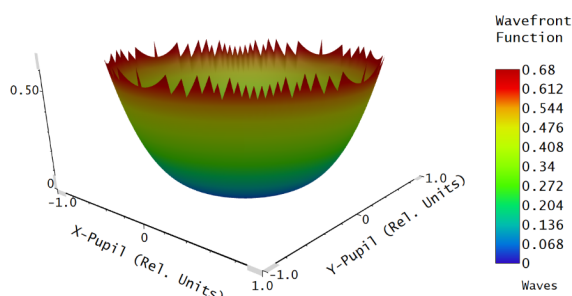


Fig. 1: Output of Zemax model of the recording system, showing  $0.67\lambda$  ( $2.85\mu\text{m}$ ) of spherical aberration.

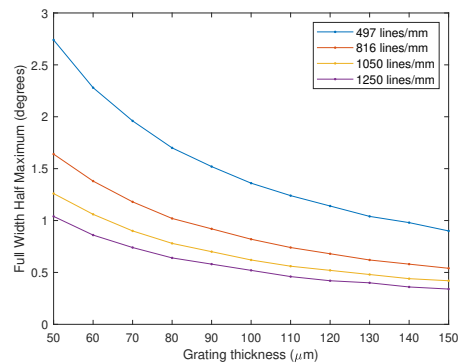


Fig. 2: Modelled grating angular selectivity, described by the Bragg diffraction efficiency curve FWHM, at various spatial frequencies & layer thickness.

The angular selectivity of gratings produced at central spatial frequencies of 497, 816, 1050, and 1250 lines/mm was examined at layer thicknesses from  $50\mu\text{m}$  to  $150\mu\text{m}$  (Fig. 2). As the spatial frequency and layer thickness were increased, it was possible to significantly increase the sensitivity of the grating to enable the detection of the small angular shift caused by the introduction of the spherical aberration. An AHWFS consisting of a HOE multiplexed with a collimated beam,  $0\mu\text{m}$ , and  $+2.85\mu\text{m}$  of spherical aberration was produced experimentally.

### 4. Conclusion

Spherical aberration induced by solely refractive elements and the angular selectivity of a holographic grating in an acrylamide-based photopolymer have been modelled. By predicting the recording conditions and grating behaviour necessary to introduce and detect a spherical aberration, we can extend the sensing capability of the AHWFS through experimental work. This has been shown for an AHWFS with a sensing range of  $0\mu\text{m}$  to  $+2.85\mu\text{m}$  of spherical aberration. Multiplexing a HOE with both defocus, as shown previously, and spherical aberration will allow for the simultaneous detection of both aberration modes by a single sensor.

### References

1. J. Schwiegerling, *Proc. SPIE*, **9186**, 91860U (2014).
2. S. Esposito et al., *Proc. SPIE*, **814902**, 8149 (2011).
3. F. Kong and A. Lambert, *Appl. Opt.*, **55**, (2016).
4. G. P. Andersen et al., *Optical Engineering*, **48**, 8, (2009).
5. A. Zepp, S. Gladysz, and K. Stein, *Advanced Optical Technologies*, **2**, (2013).
6. M. J. Booth, *Proc. SPIE*, 5162, (2003).
7. M. J. Kidger "Aberrations", in *Fundamental Optical Design*, SPIE Press, (2001).
8. M. Born and E. Wolf, "Geometrical theory of aberrations", in *Principles of Optics*, Cambridge University Press, (2003).
9. D. Vather et al., *Appl. Opt.*, **57**, 22 (2018).
10. B. Rogers, S. Martin and I. Naydenova, *Polymers*, **12**, 4, 743, (2020).
11. E. Branigan et al., *Proc. SPIE*, **11860**, 118600H, (2021).